NASA Technical Memorandum 105935
AIAA–93–0017

Effect of a Rotating Propeller on the Separation Angle of Attack and Distortion in Ducted Propeller Inlets

D.R. Boldman, C. Iek, and D.P. Hwang
Lewis Research Center
Cleveland, Ohio

and

M. Larkin and P. Schweiger
Pratt and Whitney
East Hartford, Connecticut

Prepared for the
31st Aerospace Sciences Meeting & Exhibit
sponsored by the American Institute of Aeronautics and Astronautics
Reno, Nevada, January 11–14, 1993

EFFECT OF A ROTATING PROPELLER ON THE SEPARATION ANGLE OF ATTACK AND DISTORTION IN DUCTED PROPELLER INLETS

D.R. Boldman,* C. Iek,** and D.P. Hwang**
National Aeronautics and Space Administration
Lewis Research Center
Cleveland, Ohio

M. Larkin† and P. Schweiger†
Pratt and Whitney
East Hartford, Connecticut

E-7451

Abstract

The present study represents an extension of an earlier wind tunnel experiment performed with the P&W 17-in. Advanced Ducted Propeller (ADP) Simulator operating at Mach 0.2. In order to study the effects of a rotating propeller on the inlet flow, data were obtained in the UTRC 10- by 15-Foot Large Subsonic Wind Tunnel with the same hardware and instrumentation but with the propeller removed. These new tests were performed over a range of flow rates which duplicated flow rates in the powered simulator program. The flow through the inlet was provided by a remotely located vacuum source. A comparison of the results of this flow-through study with the previous data from the powered simulator indicated that in the conventional inlet the propeller produced an increase in the separation angle of attack between 4.0° at a specific flow of 22.4 lb/sec-ft^2 to 2.7° at a higher specific flow of 33.8 lb/sec-ft^2. A similar effect on separation angle of attack was obtained by using stationary blockage rather than a propeller.

Nomenclature

A	area
C_f	friction coefficient
D	diameter
L	inlet length
M	Mach number
P	pressure
R	radius
W	mass flow rate
X	axial distance from propeller face
α	angle of attack
Θ	circumferential angle (clockwise looking downstream)
ω_{SPEC}	corrected specific flow (W_C/A_{PROP})

Subscripts

C	corrected to standard day conditions or conventional inlet
H	highlight
I	inlet
L	local condition
M	maximum value
O	freestream condition
P	plug inlet
PROP	propeller face
S	static condition or spinner
T	total condition
SEP	separated condition
1	rake station (Fig. 3)
2	propeller station (Fig. 3)

Introduction

Wind tunnel tests are often performed with inlets having an aspirated flow to simulate the flow rates

*Aerospace Research Engineer, Associate Fellow, AIAA.

**Aerospace Research Engineer, Member, AIAA.

†Research Engineer, Pratt and Whitney.

which would normally be pumped by a fan or ducted propeller in a powered simulator. A comparison of results from recent tests with the Pratt and Whitney (P&W) 17-in. Advanced Ducted Propeller (ADP) simulator in the NASA Lewis 9- by 15-Foot Low Speed Wind Tunnel (LSWT)[1] with aspirated flow test data (no propeller installed) has shown that the pumping by a propeller delays inlet separation.[2] The latter results were obtained in the UTRC 10- by 15-Foot Large Subsonic Wind Tunnel as part of a joint effort between NASA Lewis and P&W to better understand the propeller/inlet interaction problem.

Some of the concerns with past experiments of this type were eliminated in the present study through the use of the same inlet hardware, instrumentation locations, and the ability to match airflow rates in tests with and without a propeller. Past studies of this type often compared powered simulator results with data from aspirated flow tests of "similar," but not exact, geometries and instrumentation.[2] In addition to aspirated flow tests without a propeller, the program included tests to determine the feasibility of simulating the inlet angle of attack and distortion by means of stationary blockage devices which were installed in the inlet to replace the propeller.

In the present paper, experimental results from the ADP simulator and the aspirated flow studies will be compared. The aspirated flow results include data with and without the stationary blockage which was used in an attempt to simulate the effect of the propeller on the inlet distortion and separation angle of attack. Two inlets having ratios of inlet shroud length to propeller diameter of 0.53 and 0.21 were evaluated at a nominal free stream Mach number of 0.2. Predictions of the internal pressure distributions and separation angle of attack will be compared with the experimental results.

Experiments

The results presented in this paper were obtained from two independent experiments. The first experiment was performed with the 17-in. P&W ADP simulator in the LSWT. The second experiment was performed with aspirated flow in the UTRC 10- by 15-Foot Large Subsonic Wind Tunnel. The results described herein were obtained for two inlets at angles-of-attack ranging from 0° to 35° in the LSWT and from 0° to 42.6° in the UTRC wind tunnel. Although the UTRC wind tunnel could operate up to Mach 0.38, most of the tests were performed at a nominal free stream Mach number of 0.2 to coincide with the conditions in the LSWT experiments. The main emphasis of this report is to compare the inlet performance from the various tests at angles-of-attack around the separation value.

Simulator

The P&W 17-in. diameter ADP simulator is shown installed in the LSWT in Fig. 1. The simulator was laterally offset 21 in. from the centerline of the tunnel and was rotated horizontally about an aft-positioned pivot axis toward the axial centerline to provide an increase in the angle of attack. The direction of increasing angle of attack is from left to right in Fig. 1. The maximum angle of attack for the support system was 35°. The propeller was driven by a 1000 hp air turbine drive system at rotational speeds up to 12 000 rpm. At these highest rotational speeds, the corrected mass flow rate was nominally 45 lb/sec (yielding a propeller face specific flow of 35 lb/sec-ft^2). The results in Ref. 1 were primarily concerned with these high flow rate operating conditions; however, in the present paper, data from lower flow rate tests will be considered. This was necessitated because in the aspirated flow experiments at UTRC, the maximum flow rates were lower than the maximum flow rates in the simulator because of limitations imposed by the vacuum source. Further details of the simulator experiments can be obtained in Ref. 1.

Aspirated Flow

As indicated earlier, an attempt was made to circumvent some of the concerns with past experiments in which inlet tests were performed with and without a rotating propeller. Some of these concerns arose as a result of the use of similar but not exact geometries and instrumentation and from the inability to match airflow rates in tests with and without a propeller. Although the aspirated flow experiments had to be performed at lower maximum flow rates than the maximum rates in the powered simulator, there was sufficient overlap in the airflows in the two studies to allow for meaningful conclusions about flow-through and stationary blockage effects relative to propeller effects on the inlet separation angle of attack and total pressure distortion. In the aspirated flow tests with only the distortion rakes installed, corrected flow rates as high as 44.6 lb/sec could be obtained. This flow was comparable to the highest flow obtained in the powered simulator. The rakes represented a blockage of about 3 percent. When blockage devices were installed at the location of the propeller, the maximum flow rates were about 39.5 lb/sec with the highest blockage of 40 percent.

Upon completion of the experimental program in the LSWT,[1] two of the inlets and related hardware including the instrumentation rakes were transported to the UTRC 10- by 15-Foot Large Subsonic Wind Tunnel for installation and testing in the aspirated-flow mode. The aspirated inlet test setup is shown in Fig. 2. With this arrangement the inlet was rotated in the horizontal

plane (as in the simulator tests at NASA Lewis) to provide variations in angle of attack. The sweeps were made in either direction to provide a windward side which was compatible with two different rake arrangements.[2] The rakes were always installed, either at station 1 or 2, as shown in Fig. 3. The distortion results were obtained with the rakes located at station 1 in the arrangement shown in Fig. 3. The rake positions are standardized to the positions in which 0° represents the leeward side and 180° represents the windward side when viewed clockwise looking downstream. This arrangement, which coincided with the simulator setup, consisted of four long 12-element rakes circumferentially positioned at 0° (leeward side), 20°, 170°, and 185° (closest to the windward side). In addition, four 9-element boundary layer rakes were positioned at 45°, 200°, 270°, and 340°. The measurements from these rakes coupled with an assumption of symmetry about the 0° to 180° axis and an interpolation program were used to estimate the total pressure contours. The inlet rakes were located 3.0 and 2.4 in. upstream of the propeller face plane in the conventional and plug inlets, respectively. A description of the inlets will be provided later. Additional details concerning the rake element positions and data reduction procedures related to the aspirated-flow study can be obtained from Ref. 2.

Inlets

Two inlets having ratios of shroud length to propeller diameter, L_I/D_{PROP}, of 0.53 and 0.21 were tested with aspirated flow. These inlets, shown in Fig. 4, were referred to as the conventional or baseline inlet and the plug inlet. The latter inlet represented an aggressive design in terms of a short inlet forebody and diffuser length whereas the conventional inlet was more representative of contemporary designs which often contain acoustic treatment. The two inlets, shown in Fig. 4, represent the longest and shortest of a series of inlets tested in the LSWT. Results of experimental and theoretical performance for an intermediate length inlet, which was tested only with the simulator in the wind tunnel, are presented in Refs. 1 and 3. As shown in Fig. 4, different spinners were used with each inlet. The diameter of each spinner was the same in the plane of the propeller face (diameter of 17.25 in.) yielding a hub-to-tip ratio of 0.44. A short 7.9-in. spinner was used with the conventional inlet whereas a long 11.2-in. spinner was used with the plug inlet.

The two inlets contained from 38 to 50 surface static pressures, as indicated in Fig. 3, with most of these pressures concentrated in the internal portion of the inlet. Each inlet had a row of static pressure taps at the 180° circumferential position (windward side of the inlet). These pressures were used to determine the onset of separation which will be described later. The windward static pressures also provided a database for comparison with predicted pressures and separation.

Stationary Blockage Devices

In an effort to simulate the effects of the propeller on the inlet separation angle of attack and distortion, stationary blockage devices were installed in the inlet in place of the propeller. The motivation for this study was to determine the feasibility of performing inlet tests without the complexity of a powered propeller. Several blockage configurations were tested[2] including screens, rods, and combinations of rods and screens. The best simulation of powered rig inlet separation angle of attack was obtained with blockage geometries of the type shown in Fig. 5. These configurations comprised a combination of tapered rods and screens to provide a nominal blockage of 38 percent at the propeller-face plane. The rods were designed to choke the flow in the propeller-face plane at the maximum airflow operating condition.

A one-dimensional calculation was used to determine the critical area at the propeller face less the blockage of the rods, screens, and instrumentation rakes. This area was corrected to account for an empirical flow coefficient of 0.92 observed in previous testing. The area of an individual rod was the total rod blockage area divided by the number of rods needed. A conical shape was used to provide a radially uniform flow area. The inner and outer rod diameters provided equal circumferential blockage at the end walls. The notches in the rods shown in Fig. 5 merely depict adjusting screws used for installation purposes. These notches were covered to give a continuous tapered contour during testing.

A comparison of results from the flow-through (no blockage) and powered simulator tests indicated that the simulator delayed separation to higher angles of attack by more effectively pumping the region in the inlet where separation occurs. Therefore, when selecting the configurations for blockage studies, an attempt was made to redistribute the inlet flow by providing a more open path in the region where separation was expected to occur and a more restricted flow path at other circumferential positions. In the best-performing blockage devices of the type shown in Fig. 5, a hole was provided in the region where flow separation had been observed in the powered simulator tests. This hole, which extended about 90° in the circumferential direction, was formed by removing three of the tapered rods. Screen patches were placed over the remaining rods to compensate for reduced blockage resulting from the removal of the rods.

Results

Determination of Separation

The inlet separation angle of attack, α_{SEP}, was determined by the method described in Ref. 1. This method was based on experimentally varying the angle of attack in 1° increments through the separation condition to determine the angle in which the highest inlet local Mach number, M_L, is observed. The local Mach number was obtained from the ratio of the measured wall static pressure to the freestream total pressure. In Ref. 1, two types of separation were identified from the characteristics of the $M_{L,M}(\alpha)$ distributions; namely, lip separation and diffuser separation. Lip separation usually occurred at peak inlet local Mach numbers greater than 1.5, whereas diffuser separation was evident at peak inlet local Mach numbers less than 1.5. In this paper, no distinction will be made between lip and diffuser separation; however, if a definite maximum in $M_{L,M}(\alpha)$ was observed it was considered to represent the conditions at the "onset" of separation. The word "onset" is used because the value of α corresponding to the maximum observed inlet local Mach number does not yet represent a separated flow condition. Since the minimum experimental resolution of angle of attack was 1°, the angle corresponding to the maximum local Mach number represents $\alpha_{SEP}+1°$. Therefore, in the presentation of results for α_{SEP}, the angle at $M_{L,M}$ will be increased by 0.5° and the results of α_{SEP} will have an uncertainty band of ±0.5°.

Distributions of $M_{L,M}(\alpha)$

The separation angle of attack for a given inlet system, i.e., simulator, aspirated flow without stationary blockage devices, or aspirated flow with blockage, was dependent on whether the distortion rakes were installed in the inlet diffuser (station 1, Fig. 3). The presence of the rakes at station 1 produced an increase in the value of α_{SEP} by about 2° when averaged over all of the tests. This can be determined typically from the $M_{L,M}(\alpha)$ distributions for the 17-in. simulator and aspirated flow with blockage devices shown in Figs. 6(a) and (b), respectively. These results were obtained at a nominal corrected flow rate, W_C, of 38.4 lb/sec. For this particular case, the presence of the rakes produced an increase in the value of α_{SEP} by 1.5° for the simulator and by 3.0° for the blockage configuration. In the following discussion of the inlet local Mach number distributions, emphasis will be placed on the results obtained with the inlet rakes at station 2 (refer to Fig. 3). Obviously, the diffuser total pressure rakes were required in order to obtain the distortion results. Therefore, in the distortion tests, the separation angle of attack was about 2° higher than the corresponding value obtained with the rakes removed from the diffuser (moved to the propeller face, station 2).

The distributions of $M_{L,M}(\alpha)$ for the three systems are shown in Figs. 7(a) and (b) for nominal corrected flow rates of 38.4 and 32.0 lb/sec, respectively. These distributions reflect the differences in separation angle of attack for the three inlet systems. The greatest differences occurred between the results from either the powered simulator or rods/screens blockage and the aspirated flow clean inlet systems. These differences ranged from about 4° to 2° over the above range of flows.

So far the results of $M_{L,M}(\alpha)$ have been presented for two corrected flows and one inlet geometry. In the following section, the observed separation angles based on the $M_{L,M}(\alpha)$ distributions will be shown for both inlets as a function of the corrected specific flow, ω_{SPEC}, and for the full range of flows with each system. The specific flow is defined as the corrected flow per unit area at the propeller face where the area was 187.7 in^2.

Separation Angle of Attack Versus Specific Flow

The variation of separation angle of attack, α_{SEP}, with corrected specific flow, ω_{SPEC}, is shown for the conventional inlet in Fig. 8. These results were obtained without the distortion rakes in the inlet. The values of α_{SEP} have an uncertainty of ±0.5°. The effect of a rotating propeller on α_{SEP} becomes apparent upon comparing the results from the powered simulator with the results obtained with aspirated flow (no propeller). Also shown are the separation angles for the aspirated flow tests with stationary blockage. These latter results were in good agreement with the separation angles obtained with the ADP simulator. Based on the distributions shown in Fig. 8, the presence of the propeller or stationary blockage resulted in an increased separation angle of attack of from 4.0° at a specific flow of 22.5 lb/sec-ft^2 to 2.7° at a specific flow of 33.8 lb/sec-ft^2.

Similar trends in separation angle of attack were observed in tests with the plug inlet; however, the results are less conclusive because of an angle of attack limit of 35° in the LSWT ADP simulator experiments. This limit, denoted by the flagged symbols in Fig. 9 was evident at all except the highest flow rates. Relative to the results in Fig. 8 for the conventional inlet, the plug inlet showed a larger difference between the diffuser separation angles with stationary blockage devices and the separation with low blockage aspirated flow. For example, the difference in α_{SEP} was 6.3° at a specific flow of 26.85 lb/sec-ft^2 which is about 3° higher than the difference observed with the conventional inlet at the same flow rate. Based on the limited range of blockage

data, it cannot be determined whether the difference in α_{SEP} diminished at higher flow rates as it did in the conventional inlet. However, if one assumes that the stationary blockage devices were simulating the effect of the propeller on α_{SEP} as in the conventional inlet, a distribution denoted by the dashed line in Fig. 9 can be constructed. The data for this distribution include both the results with the blockage devices and the three data points from the ADP simulator tests at high values of ω_{SPEC}. Unfortunately, this assumption cannot be validated on the basis of the limited data base for the plug inlet; however, as shown in Fig. 9, separation did not occur in the simulator up to an angle of 35° over most of the flow range. These facility-limited data are denoted by the flagged symbols. The actual values of α_{SEP} are expected to be near the values obtained with stationary blockage as in the experiments with the conventional inlet. The results for the plug inlet, as extrapolated in Fig. 9, suggest a diminution of the effect of the propeller on the separation angle as the flow rate increases which is consistent with the results for the conventional inlet. At the highest specific flow of 34.2 lb/sec-ft^2 for the aspirated flow inlet without blockage devices, the difference in α_{SEP} was 2.7°.

In both inlets, the inclusion of a rotating propeller or stationary blockage device resulted in an increase in separation angle of attack relative to the aspirated-flow clean inlet operating at the same flow rate. One can postulate that the pumping of the propeller tends to energize the diffusing boundary layer and thus delay separation. The energy exchange mechanism between the inlet boundary layer and free stream is expected to be the result of a centrifuging of air by the propeller into the cowl boundary layer. This energy exchange mechanism must be different for the stationary blockage device because the effects of rotation are not present. In this latter case it is believed that the blockage device diverts some of the air from the leeward side ($\Theta = 0°$) toward the unblocked region on the windward side ($\Theta = 180°$) and reduces the adverse pressure gradient near the propeller, thus delaying separation. Evidence of this redistribution of the flow is shown by the circumferential static pressure distributions for the two inlets presented in Fig. 10. The lower static pressure (higher velocity) on the windward side results, in part, from the redistribution of the flow by the blockage device. In the conventional inlet (Fig. 10(a)) this low pressure, high velocity flow resulting from the blockage device is evident upon comparing the distributions of static pressure for the three systems. A similar trend can be noted with the plug inlet as shown in Fig. 10(b). The interaction of this locally accelerated flow with the diffusing boundary layer produces a delay in the separation, i.e., the angle of attack must be increased in order for separation to occur. The static pressures with the propeller system are similar to the pressures in the clean inlet, yet the propeller effect results in a similar increase in the separation angle of attack. Therefore it is expected that although the energy exchange mechanisms between the free stream and boundary layer are different for stationary blockage and a rotating propeller, both systems tend to produce the same effect in terms of delaying inlet separation.

Inlet Distortion—Propeller Versus Stationary Blockage

Profiles of the total pressure distortion immediately after separation were obtained only with the conventional inlet. The best comparison was obtained at a nominal flow rate of 38.4 lb/sec (ω_{SPEC} = 29.46 lb/sec-ft^2) where α_{SEP} was the same for the ADP simulator and the aspirated flow test with the blockage device shown in Fig. 5. The separation angle of attack for both experiments was 31°. The results of this comparison are presented in Fig. 11 where it can be noted that the extent of the distorted region ($P_{T,1}/P_{T,0} < 1.0$) is about the same in the simulator and aspirated flow system with stationary blockage. However, lower total pressure ratios were evident in the tests with stationary blockage. This can also be observed in Fig. 12 which shows the total pressure profiles obtained from the distortion rakes located at circumferential positions of 170° and 185°. These profiles reveal a greater loss in total pressure when the inlet was tested with stationary blockage.

Blockage Required for α_{SEP} Simulation

It has been shown that stationary blockage devices consisting of a combination of tapered rods and screens can provide a good simulation of the separation angle of attack that would be obtained with a rotating propeller in the conventional inlet. Although it cannot be proven conclusively, the results obtained with the short plug inlet suggest that stationary blockage might also provide a good simulation of the α_{SEP} that would be measured with a propeller-driven inlet. It can be stated conclusively that the inclusion of stationary blockage in an inlet provides a better simulation of α_{SEP} than otherwise obtained from aspirated flow tests without blockage devices. Now the question arises concerning the amount of blockage required in order to obtain realistic values of α_{SEP} in aspirated flow systems. The variation of α_{SEP} with blockage, based on Ref. 2, is shown in Fig. 13. The blockage variable was based on the one-dimensional Mach number through the rods and screens. This Mach number increased with increasing blockage for a given flow rate. As shown in Fig. 13, the α_{SEP}-distribution leveled off near the value of α_{SEP} obtained with the powered simulator when the one-dimensional Mach number through the blockage device exceeded a value of

about 0.8. Different combinations of rods and screens with different blockages appeared to work equally well as long as the blockage was high enough to produce Mach numbers above 0.8 at the minimum area of the blockage.

Predicted Versus Observed Axial Static Pressure

In Ref. 1 it was shown that the axial static pressure distributions for the present inlets and others were well predicted by both panel codes and Euler flow solvers[4] at all angles-of-attack up to α_{SEP}. More rigorous calculations of the unseparated flow in a similar ADP type of inlet were provided by Iek, et al.[3] in which a full Navier-Stokes code (PARC3D) was applied with different types of boundary conditions applied at the propeller face. These latter calculations provided reasonable predictions of the inlet axial static pressure distributions at an angle of attack below α_{SEP}. To illustrate what happens near separation, the panel code method of Ref. 5 with the Douglas-Neumann potential flow solver,[6-8] and the PARC3D Euler code[9] were used to predict the axial static pressures in the conventional inlet operating with stationary blockage at a flow of 38.4 lb/sec. The experimental and theoretical static pressure distributions are shown in Fig. 14 for $\alpha = 30°$ and 31°, representing conditions just before and after separation, respectively. The experimental pressure distributions obtained in the ADP simulator with a rotating propeller have also been included in order to show the close agreement in observed static pressures in the powered simulator and aspirated flow system, even immediately after separation. The theoretical pressure distributions in Fig. 14(a) are generally in good agreement with the experiment at the angle of attack of 30° (near the onset of separation). However, differences can be noted in the predicted minimum static pressures predicted by the panel and PARC3D Euler codes. In this application the panel code predicted a lower value of the minimum static pressure than the pressure predicted by the Euler code. Since the Euler and panel methods are inviscid, it is not surprising that the pressure distributions after separation are highly inaccurate as illustrated in Fig. 14(b). The same relative differences in the predicted minimum static pressures by the two methods are also apparent for this case.

Prediction of α_{SEP}

Estimates of the separation angle of attack can be obtained by incorporating a boundary layer analysis in the Euler or panel methods. An application of the method to the ADP inlets of this investigation was provided in Ref. 1. A two-part separation model was used to estimate the separation angle of attack. One part of this model was based on experimental observations from past studies of inlets operating at high angles-of-attack and at flow rates high enough to produce locally supersonic flow in the internal lip region of the windward side of the inlet. Based on these past experiments, it was concluded that a shock-induced lip separation of the internal flow in the shroud could be expected when the Mach number reached a value of about 1.5. This limit was based on an average of the results from several inlets[10] which fell within a local Mach number band of 1.5±0.15. Often the local Mach number does not reach a value of 1.5 but separation of the boundary layer still occurs in the diffuser. The separation starts near the exit plane (propeller face) and moves upstream with increasing angle of attack. These factors were combined to provide the following simple separation model. When the local Mach number reaches a value of 1.5 (usually in the neighborhood of the highlight), the inlet is assumed to separate from the lip. If this condition is not attained, the predicted friction coefficients, based on the boundary layer analysis of Ref. 11, are examined to determine if separation occurs ($C_f = 0$). Since the panel code calculations were performed on a flow-through inlet, the calculated boundary layer could separate anywhere along the flow path. For purposes of identifying the diffusion-limited angle of attack, it was assumed that this limit is reached when the calculated separation occurs upstream of the diffuser exit. The diffuser exit represents the plane of the propeller face. Further details of this separation model can be obtained in Ref. 1. As shown previously (and in Ref. 1) the panel code, with a compressibility correction, and the Euler solvers yield about the same predictions of static pressure. Consequently, the results of the predicted separation would be approximately the same for both the Euler and panel methods providing the same boundary layer analysis is used in each method.

The predicted separation boundaries for the conventional and plug inlets are compared to the experimental results from the aspirated-flow tests and the ADP simulator in Figs. 15 and 16, respectively. It was shown in Ref. 1 for the conventional inlet and other inlets that the separation model generally yielded conservative estimates of the separation angle of attack, i.e., separation was predicted up to 3° before the observed separation in the simulator. This result can be seen in Fig. 15 for the conventional inlet. Since the aspirated-flow separation results with stationary blockage were consistent with the simulator data, the underprediction is also evident for this case. The experimental flow results without a blockage device (only rake blockage of 3 percent) are in good agreement with the predicted results. This is rather reassuring because the panel code predictions are based on a flow-through model which is consistent with the low blockage experimental model having aspirated flow.

As mentioned earlier, the results for the plug inlet were less conclusive because the separation angle of attack could not be obtained in the LSWT tests with the simulator at all but the highest flow rates (refer to Fig. 9). As shown in Fig. 16, the panel code method with a separation model yields good predictions of the aspirated-flow results with low blockage.

Summary

This study to determine the effects of a rotating propeller on the separation angle of attack and distortion in subsonic inlets represents an extension of an earlier wind tunnel experiment performed with the P&W 17-in. ADP simulator operating at a freestream Mach number of 0.2. In order to study the propeller effect on the inlet flow, data were obtained with the same hardware and instrumentation but with the propeller removed. Tests were performed over a range of flow rates which duplicated flow rates in the powered simulator test program. These flows were obtained by aspirating the air through the inlet by means of a remotely located vacuum source. A second part of the present study included an effort to simulate the effect of the rotating propeller on inlet performance by installing stationary blockage devices in the position normally occupied by the propeller.

A comparison of the results of this study with previous data from a powered simulator indicated that in the conventional inlet the propeller produced an increase in the separation angle of attack between 4.0° at a specific flow of 22.5 lb/sec-ft^2 to 2.7° at a higher specific flow of 33.8 lb/sec-ft^2. A similar effect on separation angle of attack was obtained by using stationary blockage rather than a propeller. The best stationary blockage device consisted of a special combination of tapered rods and screens. This device produced a good duplication of the separation angle of attack obtained in the powered simulator; however, the total pressure distortion pattern revealed some differences. Although the extent of the distorted region was well duplicated with blockage, the losses in total pressure in the distorted region were greater with the blockage devices than the losses in the powered simulator.

Similar trends were obtained with the shorter of the two inlets which were tested (plug inlet); however, a good quantitative comparison could not be made for this case because of certain testing limitations. The use of blockage devices in place of the propeller increased the separation angle by a maximum of 6.3° over the corresponding value obtained with aspirated flow and no blockage devices.

Observed separation angles from the aspirated flow tests were compared with the results from a coupled panel code and boundary layer calculation which incorporated a simple model for separation. The calculated separation angles-of-attack were within ±1° of the values obtained in the aspirated flow tests (without blockage).

Concluding Remarks

An important ramification of these results concerns the method in which aspirated flow tests are performed. The inclusion of stationary blockage devices to replace the propeller can provide a better simulation of separation angle of attack than the more traditional aspirated flow tests without blockage. The results of this study also suggested that total pressure distortion simulation is best achieved by conducting the tests with a powered propeller. Although the extent of the distorted flow was well duplicated with blockage, the losses in total pressure in the distortion region were greater with blockage devices than the losses observed in the powered simulator.

The experiments indicated that the separation angle of attack in a clean inlet tested with aspirated flow can be anywhere from about 2.7° to 4.0° below the values obtained in a powered simulator or aspirated flow system with blockage. Predictions of the separation angle of attack in which the propeller effect was not included yielded levels of separation angle which were consistent with the clean inlet aspirated flow results. Therefore the predictions as well as the clean inlet aspirated flow results tended to yield conservative results.

References

1. Boldman, D.R., Iek, C., Hwang, D.P., and Jeracki, R.J., Larkin, M., and Sorin, G., "Evaluation of Panel Code Predictions with Experimental Results of Inlet Performance for a 17-Inch Ducted Prop/Fan Simulator Operating at Mach 0.2," AIAA Paper 91–3354, June 1991.

2. Larkin, M., and Schweiger, P., "Ultra High Bypass-Nacelle Aerodynamics Inlet Flow-Through High Angle of Attack Distortion Test," NASA CR–189149, July 1992.

3. Iek, C., Boldman, D.R., and Ibrahim, M., "Analysis of an Advanced Ducted Propeller Subsonic Inlet," AIAA Paper 92–0274, Jan. 1992.

4. Ni, R.-H., "A Multiple Grid Scheme for Solving the Euler Equations," AIAA Paper 81–1025, June 1981.

5. Stockman, N.O., and Farrell, Jr., C.A., "Improved Computer Programs for Calculating Potential Flow in Propulsion System Inlets," NASA TM–73728, July 1977.

6. Smith, A.M.O., and Pierce, J., "Exact Solution of the Neumann Problem. Calculation of Non-Circulatory Plane and Axially Symmetric Flows About or Within Arbitrary Bodies," ES–26988, Douglas Aircraft Co., Apr. 1958.

7. Hess, J.L., and Smith, A.M.O., "Calculation of Potential Flow About Arbitrary Bodies," Progress in Aeronautical Sciences, Vol. 8, edited by D.A. Kuchemann, Pergamon Press, Elmsford, NY, 1967, pp. 1–138.

8. Hess, J.L., "Calculation of Potential Flow About Bodies of Revolution Having Axes Perpendicular to the Free-Stream Direction," Journal of the Aerospace Sciences, Vol. 29, No. 6, June 1962, pp. 726–742.

9. Cooper, G.K., and Sirbaugh, J.R., "The PARC Distinction: A Practical Flow Simulator," AIAA Paper 90–2002, 1990.

10. Luidens, R.W., Stockman, N.O., and Diedrich, J.H., "Optimum Subsonic, High-Angle-of-Attack Nacelles," International Council of the Aeronautical Sciences, Congress, 12th, Proceedings, edited by J. Singer and R. Staubenbiel, AIAA, New York, 1980, pp. 530–541.

11. Herring, H.J., "PL2—A Calculation Method for Two-Dimensional Boundary Layers with Crossflow and Heat Transfer," Dynalysis of Princeton, Report No. 65, July 1980.

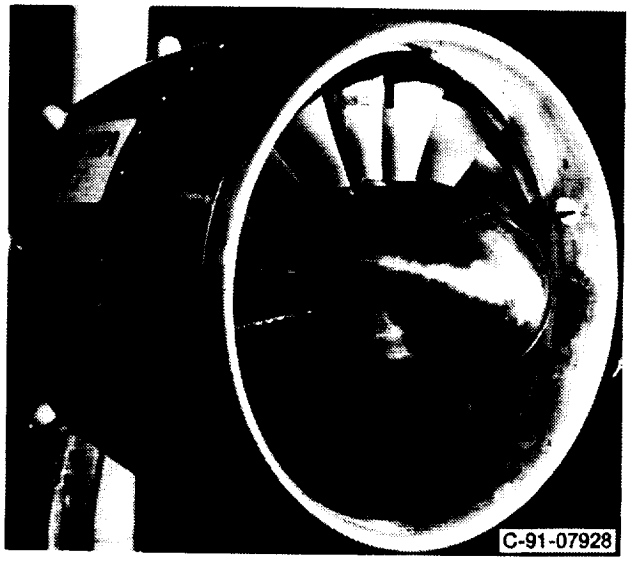

Figure 1.—P&W 17-in. diam ADP simulator installed in the NASA LeRC 9- by 15-ft Low Speed Wind Tunnel.

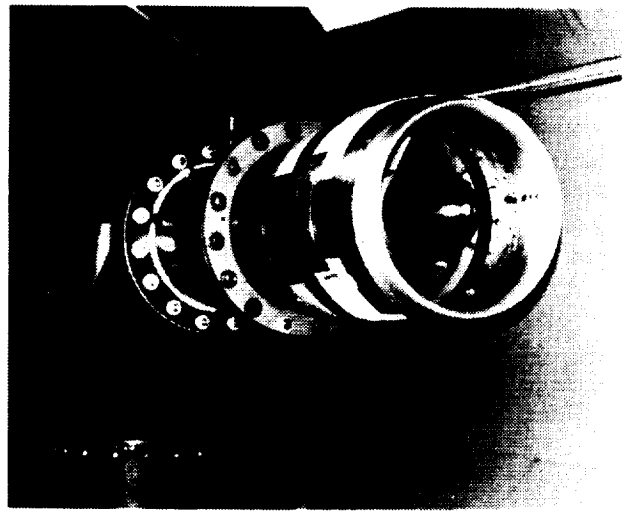

Figure 2.—Aspirated flow test setup in the UTRC 10- by 15-ft Large Subsonic Wind Tunnel.

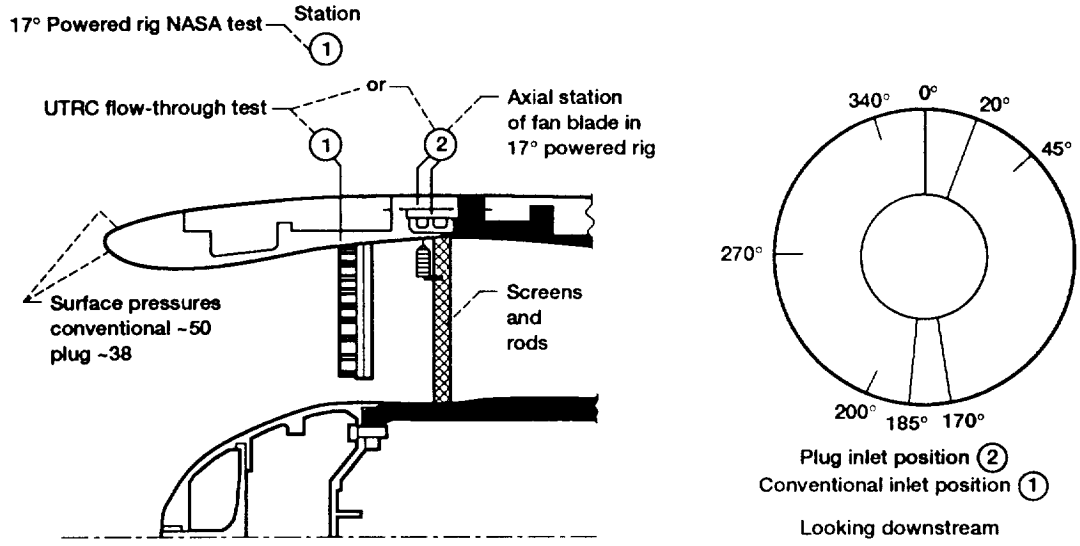

Figure 3.—Inlet total pressure rake arrangement for aspirated flow experiments.

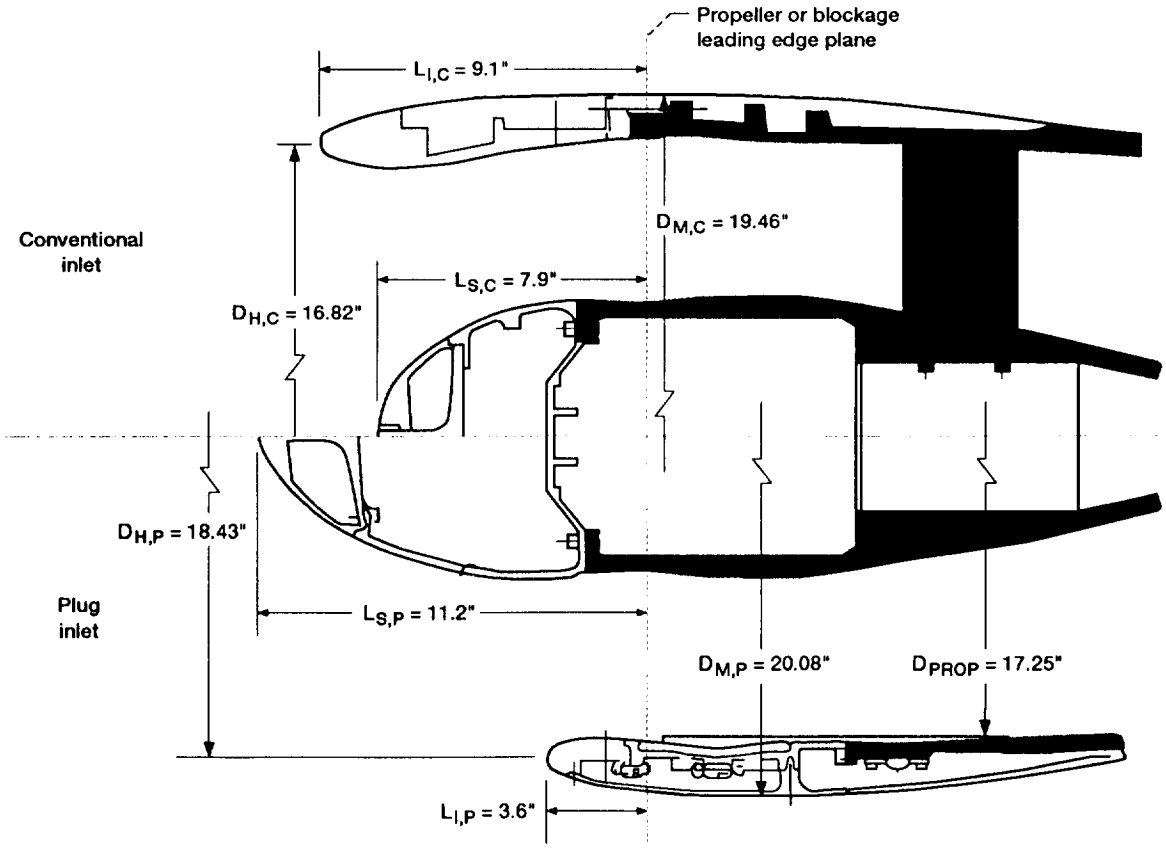

Figure 4.—ADP inlets tested with aspirated flow.

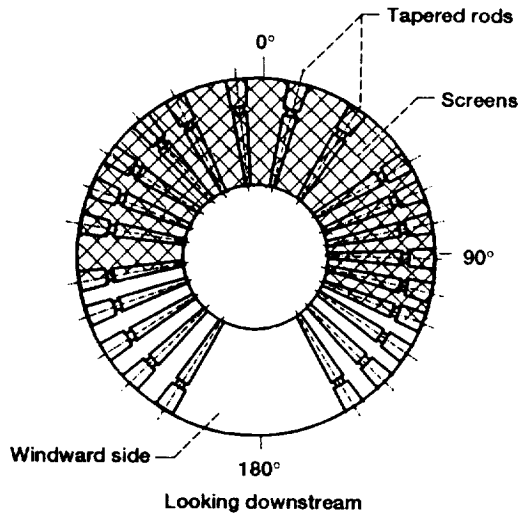

Figure 5.—Typical stationery blockage device consisting of tapered rods and screens. Nominal area blockage, 38 percent.

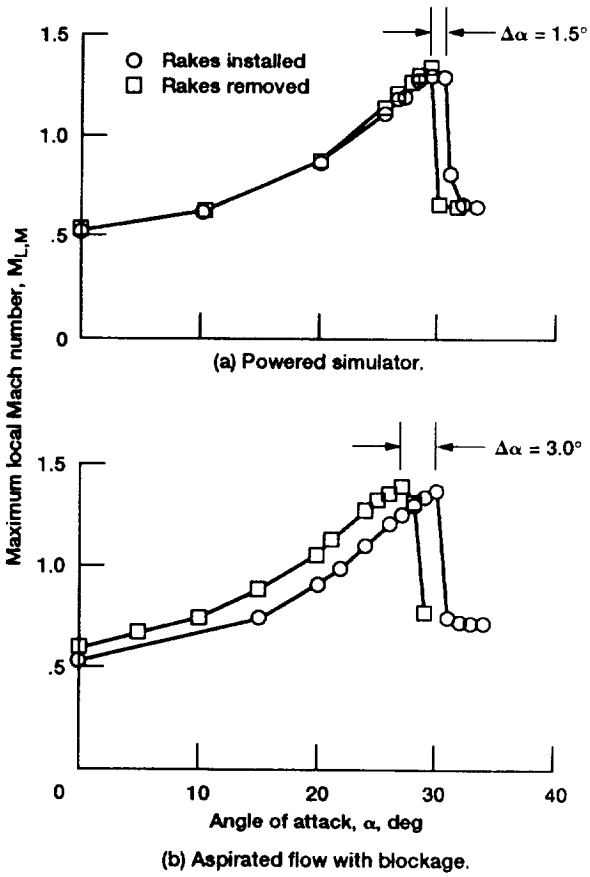

Figure 6.—Influence of inlet total pressure rakes on α_{SEP} in the conventional inlet. $M_O \approx 0.2$, $W_C \approx 38.4$ lb/sec.

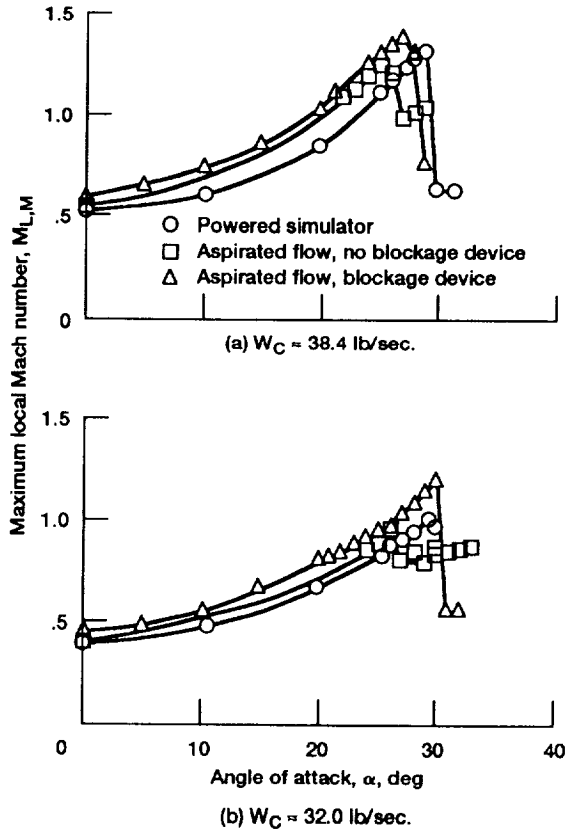

Figure 7.—Distributions of $M_{L,M}$ (α) for the conventional inlet in the powered simulator and aspirated flow system with and without stationary blockage devices. $M_O \approx 0.2$.

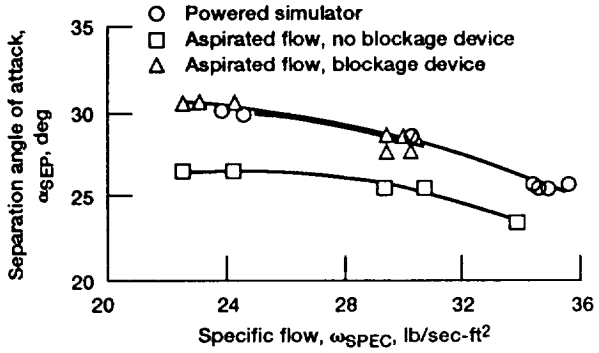

Figure 8.—Variation of α_{SEP} with ω_{SPEC} for the conventional inlet. $M_O \approx 0.2$.

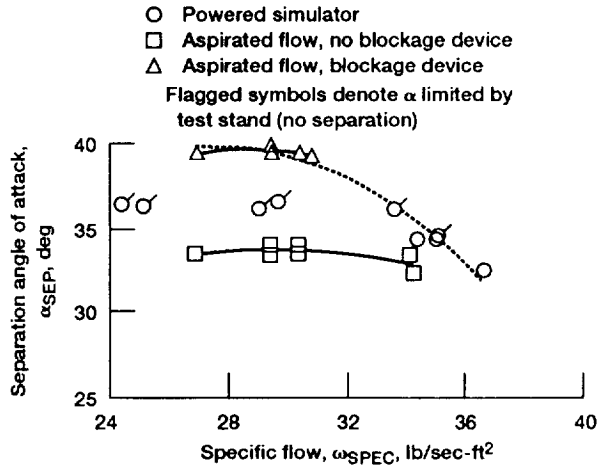

Figure 9.—Variation of α_{SEC} with ω_{SPEC} for the plug inlet. $M_O \approx 0.2$.

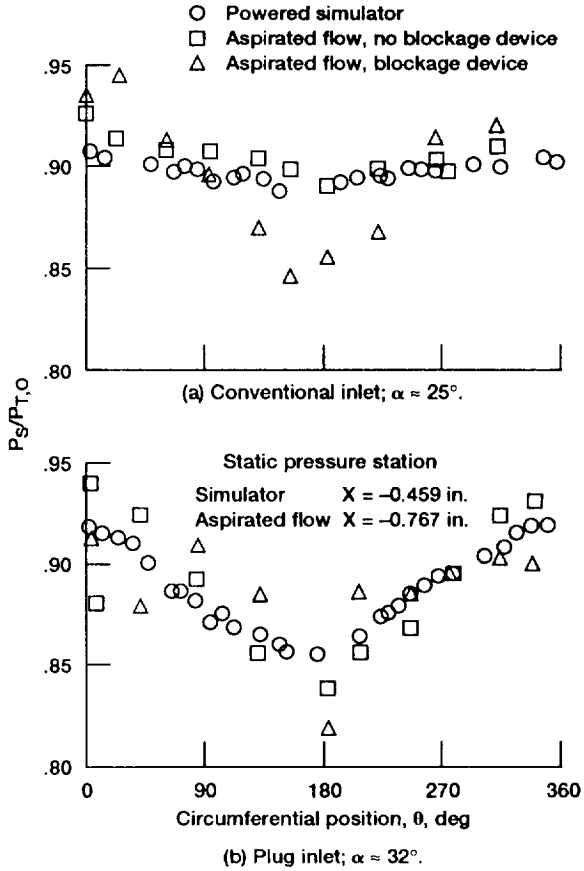

Figure 10.—Inlet static pressure distortion near the propeller face just before clean-inlet separation. $M_O \approx 0.2$; $W_C \approx 38.4$ lb/sec.

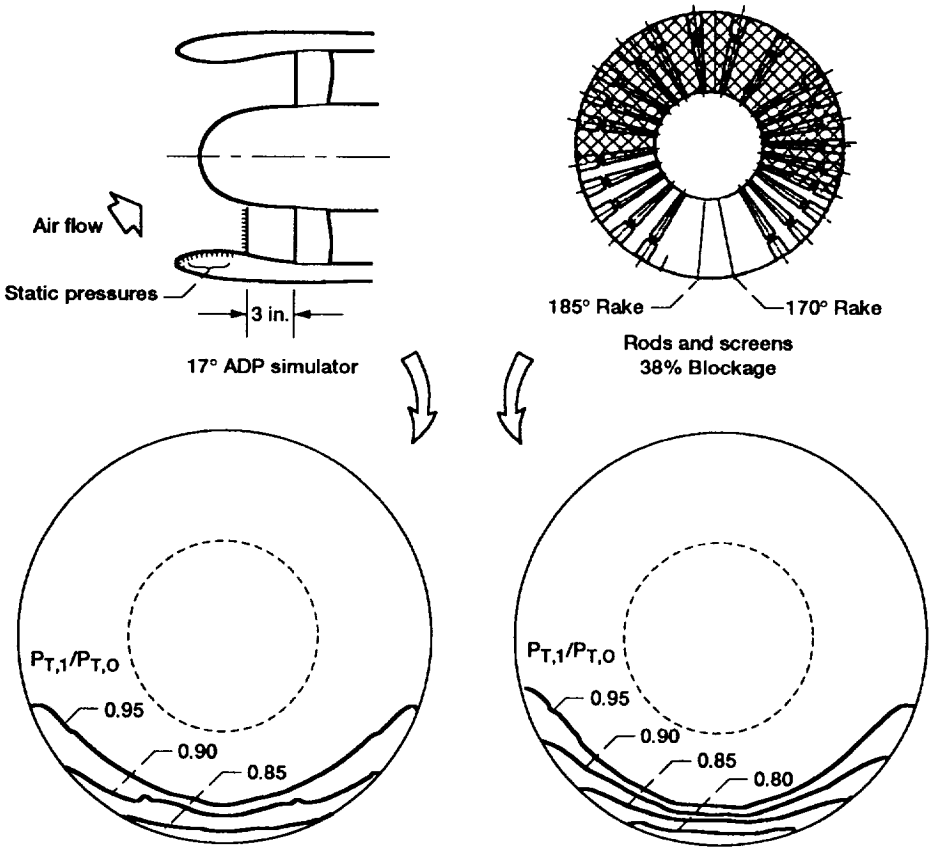

Figure 11.—Comparison of total pressure distortion in the conventional inlet operating with the powered simulator and as an aspirated-flow system with blockage. $M_O \approx 0.2$; $W_C \approx 38.4$ lb/sec; $\alpha \approx 31°$.

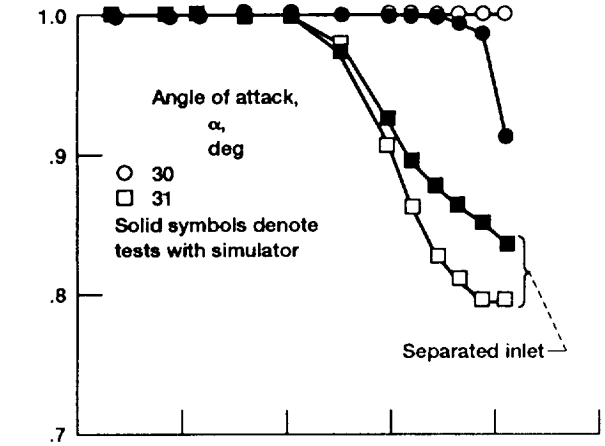

(a) 185° Rake.

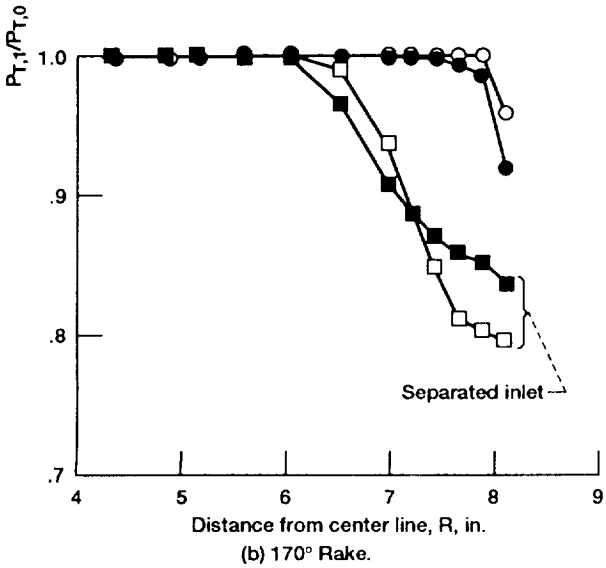

(b) 170° Rake.

Figure 12.—Comparison of radial distributions of total pressure near windward side in conventional inlet operating with the powered simulator and as an aspirated flow system with blockage. $M_0 \approx 0.2$; $W_c \approx 38.4$ lb/sec.

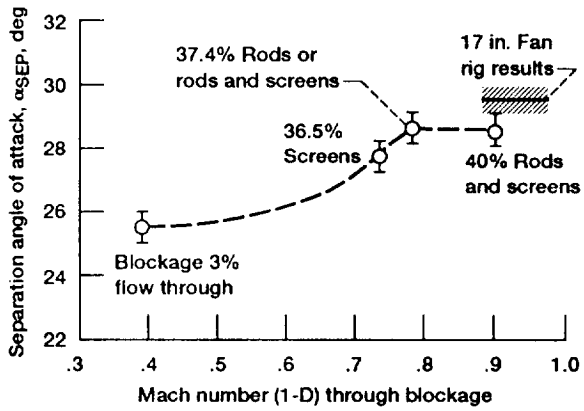

Figure 13.—Variation of α_{SEP} with blockage Mach number in the conventional inlet. $M_O \approx 0.2$; $W_C \approx 38.4$ lb/sec.

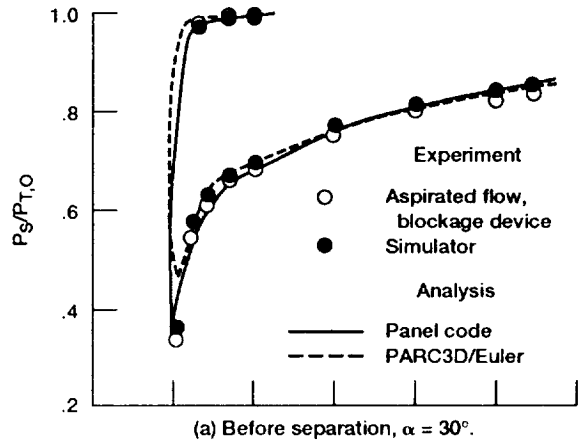

(a) Before separation, $\alpha = 30°$.

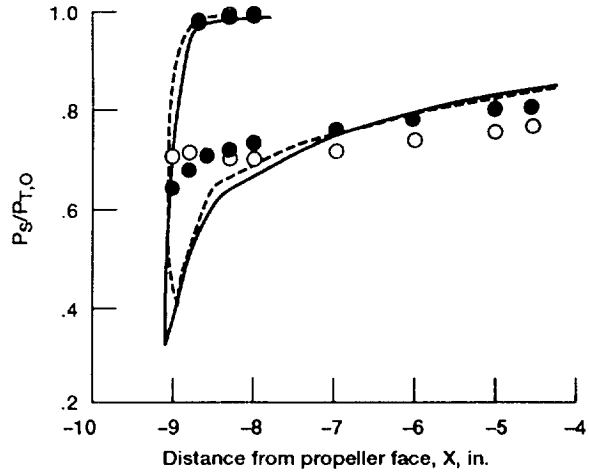

(b) After separation, $\alpha = 31°$.

Figure 14.—Predicted static pressure distributions in the conventional inlet before and after separation. $M_O \approx 0.2$; $W_C \approx 38.4$ lb/sec; $A_{PROP} = 187.7$ in^2.

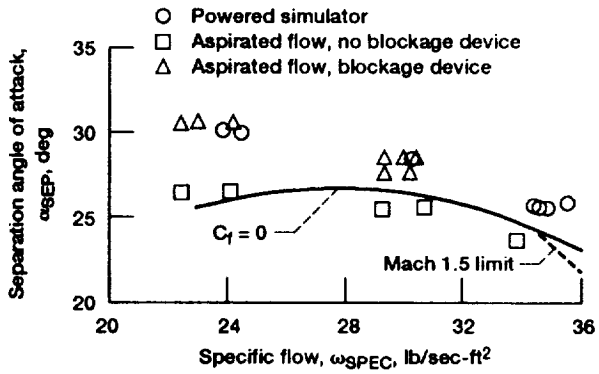

Figure 15.—Comparison of predicted and observed separation in the conventional inlet operating with the powered simulator and as an aspirated-flow system with and without blockage. $M_O \approx 0.2$; $A_{PROP} = 187.7$ in^2.

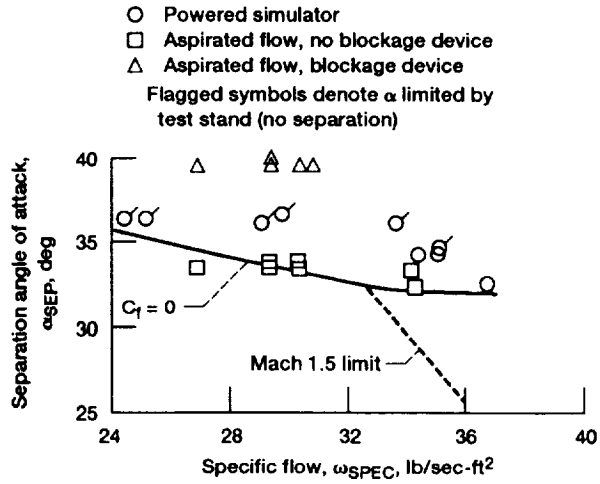

Figure 16.—Comparison of predicted and observed separation in the plug inlet operating with the powered simulator and as an aspirated-flow system with and without blockage. $M_O \approx 0.2$; $A_{PROP} = 187.7$ in^2.

REPORT DOCUMENTATION PAGE

Form Approved
OMB No. 0704-0188

1. AGENCY USE ONLY (*Leave blank*)	2. REPORT DATE	3. REPORT TYPE AND DATES COVERED
	January 1993	Technical Memorandum

4. TITLE AND SUBTITLE

Effect of a Rotating Propeller on the Separation Angle of Attack and Distortion in Ducted Propeller Inlets

5. FUNDING NUMBERS

WU-505-03-10

6. AUTHOR(S)

D.R. Boldman, C. Iek, D.P. Hwang, M. Larkin, and P. Schweiger

7. PERFORMING ORGANIZATION NAME(S) AND ADDRESS(ES)

National Aeronautics and Space Administration
Lewis Research Center
Cleveland, Ohio 44135-3191

8. PERFORMING ORGANIZATION REPORT NUMBER

E-7451

9. SPONSORING/MONITORING AGENCY NAMES(S) AND ADDRESS(ES)

National Aeronautics and Space Administration
Washington, D.C. 20546-0001

10. SPONSORING/MONITORING AGENCY REPORT NUMBER

NASA TM-105935
AIAA-93-0017

11. SUPPLEMENTARY NOTES

Prepared for the 31st Aerospace Sciences Meeting & Exhibit sponsored by the American Institute of Aeronautics and Astronautics, Reno, Nevada, January 11-14, 1993. D.R. Boldman, C. Iek, and D.P. Hwang, NASA Lewis Research Center, Cleveland, Ohio. M. Larkin and P. Schweiger, Pratt and Whitney, East Hartford, Connecticut. Responsible person, D.R. Boldman, (216) 433-3692.

12a. DISTRIBUTION/AVAILABILITY STATEMENT

Unclassified - Unlimited
Subject Category 02

12b. DISTRIBUTION CODE

13. ABSTRACT ***(Maximum 200 words)***

The present study represents an extension of an earlier wind tunnel experiment performed with the P&W 17-in. Advanced Ducted Propeller (ADP) Simulator operating at Mach 0.2. In order to study the effects of a rotating propeller on the inlet flow, data were obtained in the UTRC 10- by 15-Foot Large Subsonic Wind Tunnel with the same hardware and instrumentation but with the propeller removed. These new tests were performed over a range of flow rates which duplicated flow rates in the powered simulator program. The flow through the inlet was provided by a remotely located vacuum source. A comparison of the results of this flow-through study with the previous data from the powered simulator indicated that in the conventional inlet the propeller produced an increase in the separation angle of attack between 4.0° at a specific flow of 22.4 lb/sec-ft^2 to 2.7° at a higher specific flow of 33.8 lb/sec-ft^2. A similar effect on separation angle of attack was obtained by using stationary blockage rather than a propeller.

14. SUBJECT TERMS	15. NUMBER OF PAGES
Engine inlets; Subsonic inlets; Inlet distortion; Shrouded propellers; Separation	16
	16. PRICE CODE: A03

17. SECURITY CLASSIFICATION OF REPORT	18. SECURITY CLASSIFICATION OF THIS PAGE	19. SECURITY CLASSIFICATION OF ABSTRACT	20. LIMITATION OF ABSTRACT
Unclassified	Unclassified	Unclassified	